Arabian Journal of Geosciences (2023) 16:448
https://doi.org/10.1007/s12517-023-11566-z

ORIGINAL PAPER

The Paleocene climate in west central Sinai (Egypt): insights from the calcareous nannofossils

Mahmoud Faris[1] · Manal Shabaan[1] · Ahmed Awad Abdelhady[2,3] · Mohamed S. Ahmed[4] · Fatma Shaker[5]

Received: 21 March 2023 / Accepted: 17 June 2023

Abstract

To reconstruct the paleoclimate in North Africa during the Paleocene, the calcareous nannofossils were quantitatively analyzed at higher resolution from the stratigraphic succession of Gebel Nezzazat (west central Sinai, Egypt). The studied interval extends from NP4 to NP8. Zone NP4 can be subdivided into four subzones from base to top: NTp7B, NTp8A, NTp8B, and NTp8C. The base of the Selandian age is located at the base of NTp8B (Second Radiation of Fasciculithus). The Selandian/Thanetian boundary (S/T) is tentatively placed at the base of Zone NP7/8. The identified nannofossil zones were compared with that of the Tethyan region for the Danian/Selandian boundary. The calcareous nannofossil assemblages were used as indicators for medium-term climatic fluctuations. The pre-Danian (LDE) is dominated by the cool-water *Zeugrhabdotus sigmoides* and *Neochiastozygus modestus*, while the post-Danian interval is dominated by *Coccolithus pelagicus* and *Ericsonia subpertusa*. Before the onset of the Selandian-Thanetian boundary, a marked shift in the nannofossil species was observed, where Fasciculithus increased significantly, while marker Danian-Selandian genera (e.g., *Lithoptychius Neochiastozygus*, *Chiasmolithus*, and *Cruciplacolithus*) decreased dramatically. Non-Metric Multidimensional Scaling (nMDS) and permutational analysis of variance (PERMANOVA) in addition to the Temperature and Nutrient indices (TI and NI) indicated a marked difference between the warm eutrophic nannofossil assemblages at the Danian/Selandian (D/S) and the Selandian/Thanetian (S/T) transitions and the eutrophic cold-water assemblages during the background sedimentation. A sharp increase in sea surface temperature and decrease in nutrients was observed at D/S and represents the Latest Danian Event (LDE), while the second warming event was started prior to the Selandian and may represent the Early Late Paleocene Event "ELPE." The sea-level lowstand may have limited water circulation, where surface water fertility decreased significantly. Consequently, nannofossil diversity decreased. The rapid recovery after the LDE was attributed to the radiation of warm-water taxa.

Keywords Calcareous nannofossils · Paleocene hyperthermal · Danian/Selandian · Southern Tethys

Introduction

The Paleocene epoch is bounded by two major events in the earth's history, namely, the Cretaceous-Paleogene mass extinction (K/Pg) caused by a bolide impact and intensive volcanism and the Paleocene–Eocene Thermal Maximum (PETM), a spike in global temperatures and ocean acidification (Keller et al. 2018; Schoene et al. 2019; Elewa and Abdelhady 2020a, b). In the last few years, many investigations indicate that the PETM was preceded by many similar (but with different magnitudes) hyperthermal events throughout the Paleocene (Arreguín-Rodríguez et al. 2016).

Several records indicated a long-term global cooling trend initiated at about 63.0 Ma and continued to the Early Late Paleocene Event (ELPE) event at the base of Thanetian (~ 58.5 Ma), with a steady increase in the

Responsible Editor: Attila Ciner

✉ Ahmed Awad Abdelhady
ahmed.abdelhady@mu.edu.eg

[1] Faculty of Science, Department of Geology, Tanta University, Tanta, Egypt

[2] Geology Department, Faculty of Science, Minia University, El–Minia 61519, Egypt

[3] Department of Palaeontology, University of Vienna, Althanstrasse 14, 1090 Vienna, Austria

[4] Geology and Geophysics Department, College of Science, King Saud University, 2455, Riyadh 11451, Saudi Arabia

[5] Faculty of Science, Department of Geology, Benha University, Benha 13518, Egypt

Published online: 04 July 2023

rate of sedimentation and carbonate production (Westerhold et al. 2008). The cooling trend was interrupted by a transient warming of more than 2 °C at 61.75 Ma, which marks the onset of the Paleocene carbon isotope maximum (PCIM; Shackleton et al. 1984; Hilting et al. 2008). In addition, these hyperthermal events include also the Latest Danian Event "LDE" (Bornemann et al. 2009; ~61.75 Ma), the Danian/Selandian transition event (Speijer 2003; ~61 Ma), the ELPE (Röhl et al. 2004; Bralower et al. 2005), or the Mid-Paleocene Biotic Event "MPBE" (Bernaola et al. 2007; ~58.2 Ma). However, the magnitude and geographic range of these "events" is still a matter of debate (Westerhold et al. 2011). This problem is exaggerated by the scarcity of complete stratigraphic records due to global lowstand sea level. Data are still too sparse to conclude that the ELPE was a global hyperthermal-type event.

The Danian/Selandian (D/S) boundary was suggested to be the earliest episode of global warming after the Cretaceous/Paleogene boundary (K/Pg) event and before the most known of the Paleocene/Eocene Thermal Maximum (PETM; 55 Ma, Zachos et al. 2003). The D/S boundary is marked by global oceanic changes reflected in major faunal turnover (e.g., Speijer 2003; Guasti et al. 2005). More recently numerous studies have been conducted in the Tethyan Realm to redefine the Global Stratotype Section and Point (GSSP) of the D/S boundary in more complete stratigraphic sections (Monechi et al. 2013; Alegret et al. 2016; Metwally 2019).

Denmark is home to the type locations for the Danian and Selandian stages. In this area, the D/S boundary is characterized by an unconformity between the Danskekalk Formation and the Lellinge Formation (Thomsen and Heilmann-Clausen 1985). In the recent few years, the Danian-Selandian boundary has been formally defined in the Zumaia section in Spain (Schmitz et al. 2011), and the biostratigraphical resolution of this interval has been refined (Agnini et al. 2007; Arenillas et al. 2008; Bernaola et al. 2009; Sprong et al. 2009).

Despite these investigations in the past few years and according to Alegret et al. (2016), paleoenvironmental characteristics of the Paleocene hyperthermal events rather than the PETM are poorly understood, and further investigations are necessary to characterize these minor hyperthermal events in the Paleogene. Therefore, we aim herein to exploit the nannofossil-rich succession Gebel Nezzazat to (1) estimate the exact time, magnitude, and pattern of Paleocene hyperthermal events on the nannofossils (the D/S boundary and the S/T boundary), and (2) reconstruct the paleoclimate of the Paleocene in Norther Africa based on quantitative analyses of the nannofossils distribution. Quantitative analyses of the nannofossils were approved to be highly valuable in paleoenvironmental reconstructions (Kassab and Abdelhady 2022; Jain et al. 2022).

Stratigraphic framework

During the Paleocene, a vast area of Egypt was covered by epicontinental basins, where marine shelf carbonates and deltaic sediments were accumulated along these basins (Speijer 2003; Elewa and Abdelhady 2020a, b; Sayed et al. 2022), which are outcropping now at the eastern side of the Gulf of Suez (Fig. 1). The Paleocene succession of the study section spans the upper part of the Dakhla and the Tarawan formations (Fig. 2). The Paleocene succession is composed mainly of marls and limestone sediments rich in planktic foraminifera and calcareous nannofossils, which indicates an open setting and direct connection with the Western Tethys (Speijer 2003).

The Dakhla Formation (Said 1962) composes of gray shale alternated with some marls at Wadi Nezzazat sections; it is overlain by the Tarawan Formation, which is mainly composed of chalk. In the G. Nezzazat section, the studied part of this formation attains a thickness of about 12.5 m. In the G. Nezzazat section, dark brown shale-marl thin beds rich in organic carbon, coprolites, and fish remains is representing the P/E Event within the Dakhla Formation (bed, about 1.5 m, samples 7–11, Fig. 2). Awad and Ghobrial (1965) studied the succession of Gebel Tarawan in Kharga Oasis and introduced the Tarawan Formation, which is composed of chalk, chalky limestones, and marly limestone upward. The investigated part of this formation in our study is about 1.75 m. It is underlain by the shale of the Dakhla Fm and consists mainly of hard white chalky limestone (Fig. 2). It was assigned a Thanetian Age.

Material and methods

Sampling

Nearly complete section across the D/S boundary was studied at G. Nezzazat section located in the west central Sinai and bounded between latitudes 28°47′45.4″N and longitudes 33°14′9.79″E (Fig. 1). The study section was located in the arid zone during the Paleocene (Fig. 1). Forty-one rock samples were collected at 5 cm intervals vertically from the sediments encompassing the D/S boundary, while the space interval ranges from 1 to 10 m below and above this boundary (Fig. 2). The settling preparation procedure was used to prepare nannofossil smear slides (Perch-Nielsen 1985) using a Zeiss light microscope with × 1250 magnification, to identify calcareous nannofossil biozones and for counting the most important biostratigraphic markers throughout the studied interval. The code of abundance and preservation are as follows: A

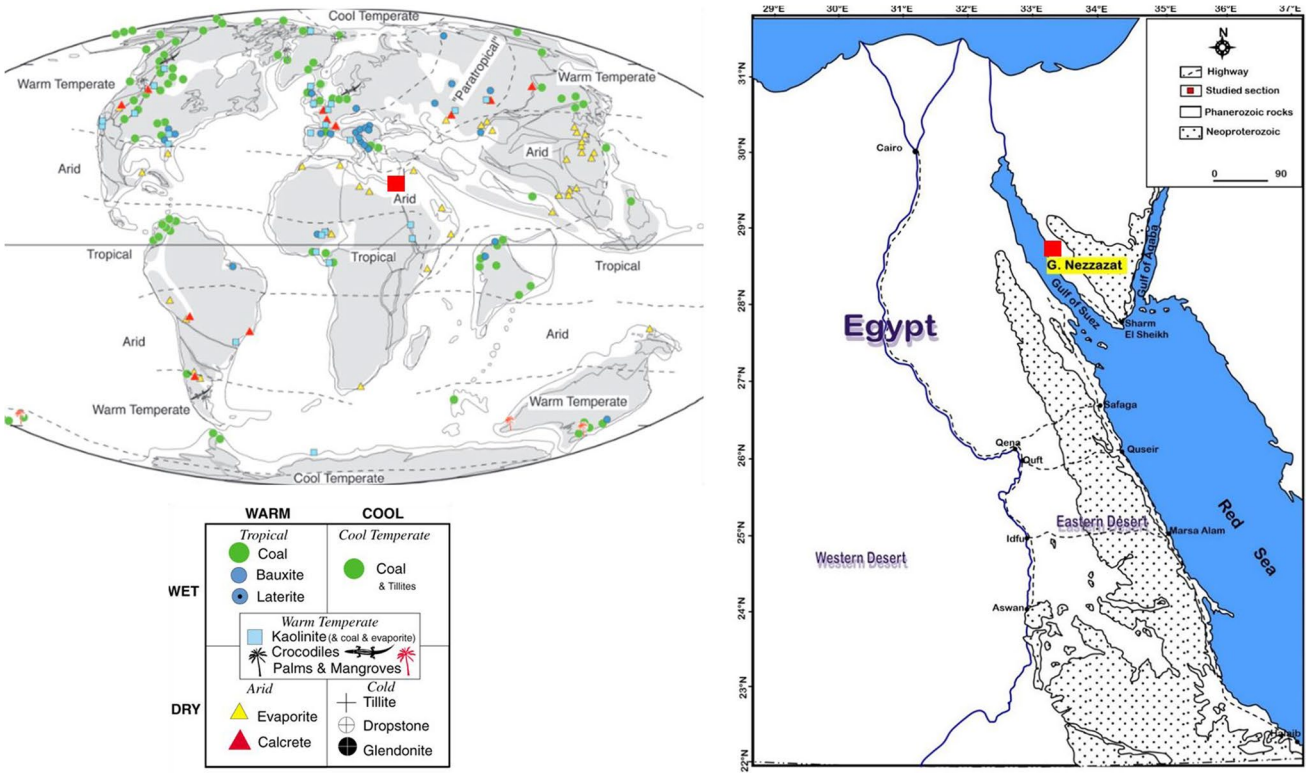

Fig. 1 Location of the studied section (G. Nezzazat) on a paleoclimate map of the Paleocene (after Boucot et al. 2013). The study area is located in the arid zone in the Western Tethys

(abundant), more than 10 specimens/field of view (FOV); C (common), one to ten specimens/FOV; F (few), one specimen/one to ten FOV; R (rare), one specimen/eleven to twenty/FOV; VR (very rare), one specimen/more than twenty/FOV. Only a few specimens showed signs of dissolution and/or overgrowth, indicating that preservation of the taxa is moderate to good. In each slide, 300–400 individuals were counted (Appendix A).

Nannofossil indices

The relative abundances of species in the samples and assemblages and the diversity indices (Shannon, Evenness, and Dominance) were calculated and used to assess the response of the nannofossils to environmental stress. The paleoecological significance of the calcareous nannofossils (Nutrient index, Temperature index) is estimated based on the following equations: The Nutrient index NI = {SUM (% of Meso-eutrophic taxa)/(% of Meso-eutrophic taxa + % of oligotrophic taxa)*100} (Appendix B). The Temperature index TI = {SUM (% of cold taxa)/(% of cold taxa + % of warm taxa)*100} (Appendix C). Species preferences were compiled from literature (e.g., Bralower 2002; Bernaola et al. 2007; Mutterlose et al. 2007; Raffi et al. 2009; Clark and Watkins 2020; Kassab et al. 2022; Shaker and Kassab 2022; Kasem et al. 2022) (Appendix B and C).

Statistics

The final species-sample matrix includes 41 nannofossil samples containing 443,131 specimens of 48 species were subjected to quantitative analyses. To identify the nannofossil assemblages, the UPGMA (Unweighted Pair Group Method with Arithmetic Mean) clustering was applied using Bray–Curtis similarity (Clarcke 1993). The Cophenetic Correlation Coefficient (CCC) was used to evaluate the quality of the dendrograms. In this case, CCC = 0.883, which indicates good quality of the resulting dendrogram. We grouped the samples based on their stratigraphic positions (zones and subzones). Then, the Non-Metric Multidimensional Scaling (nMDS) based on Bray–Curtis similarity was used to visualize the differences among these assemblages. The goodness of fit for the nMDS was assessed by the stress value, where stress < 0.2 is good (herein, the stress = 0.13; which indicates very good quality of fit; Legendre and Legendre, 1983). The degree of the overlap among the objects on the NMDS plot gives hints about the relationship among these objects; however, this can vary among different authors. Therefore, the permutational analysis of variance (PREMANOVA)

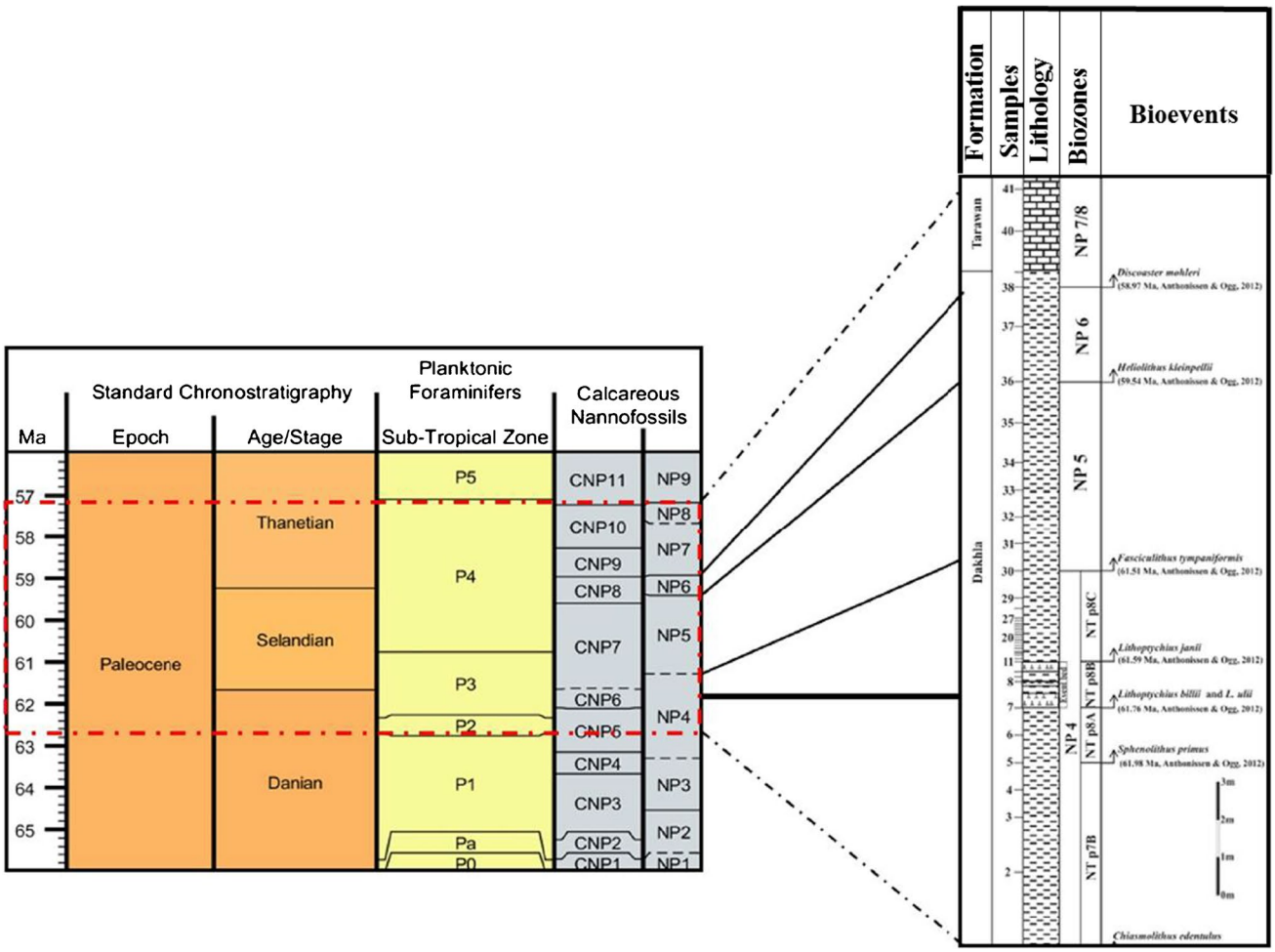

Fig. 2 Stratigraphic chart of the Paleocene succession at G. Nezzazat west central Sinai, Egypt. The chalk of the Tarwan Formation (NP7-8) overlains the Dakhla Formation, which composed mainly of argillaceous sediments. The D/S boundary is located at the base of the NTp8c

test was used to test the significance of the relationships among the identified assemblages. The Sequential Bonferroni correction was used to govern significant differences at p level = 0.001 (Hammer and Harper 2006). Reduced Major Axes (RMA) regression was used to identify the relationships among the dominated species and nannofossil indices. Box plots were used to figure out differences among assemblages. All statistical analyses were carried out using the PAST V. 2.17 (Hammer et al. 2001).

Results

Nannofossil biostratigraphy

A quantitative calcareous nannofossil investigation was carried out on the event interval from the study section. Calcareous nannofossils are moderate to well-preserved and quantitively rich and very diverse. The standard calcareous nannofossil zonal schemes of Martini (1971) and Varol (1989) were used in this study. The bioevents were correlated with other studies of the Tethyan region. Abbreviations used are HO = highest occurrence, LO = lowest occurrence, and LCtO = lowest consistent occurrence. The index species are illustrated on one plate (Fig. 1). The relative abundance (in percent), for some stratigraphically important nannofossils taxa, is illustrated in Tables 1 and 2. Some important remarks for the different biozones and subzones are briefly given below.

Ellipsolithus macellus Zone (NP4).

This zone includes the interval from the lowest occurrence (LO) of *E. macellus* to the LO of *F. tympaniformis* (Appendix A). *Ellipsolithus macellus* shows a very rare distribution in the study section. This zone can be divided into two zones (NTp7 and NTp8) and four (NTp7B, NTp8A, NTp8B, and NTp8C) subzones utilizing Varol (1989). These subzones are explained and addressed in the following sections, from the older to the younger.

Table 1 Assemblages of each section. Significant values are in bold (Sequential Bonferroni corrected *p* value)

Nannofossil zone	Thanetian	Selandian				Danian	
	NP7/8	**NP6**	**NP5**	**NT p8C**	**NT p8B**	**NT p8A**	**NT p7B**
NP7/8	0						
NP6	0.1348	0					
NP5	0.0045	0.0375	0				
NT p8C	**0.0003**	0.005	**0.0002**	0			
NT p8B	0.0291	0.0666	0.0041	**0.0004**	0		
NT p8A	0.0644	0.3358	0.0356	0.0047	0.0729	0	
NT p7B	0.0285	0.069	0.0059	**0.0001**	0.0267	0.064	0

Table 2 Comparison among the biotic traits of the identified nannofossil assemblages

	NP7/8	**NP6**	**NP5**	**NT p8C**	**NT p8B**	**NT p8A**	**NT p7B**
Species	14	12	15	19	20	14	10
Individuals	322	306	346	378	397	359	329
Dominance	0.09	0.10	0.08	0.06	0.06	0.08	0.12
Shannon	2.53	2.40	2.57	2.85	2.87	2.54	2.18
Evenness	0.93	0.93	0.92	0.92	0.90	0.94	0.91
Oligotrophic taxa	72.82	78.51	54.11	36.06	52.23	28.80	18.21
Meso-Eutrophic taxa	21.58	19.88	35.91	47.35	33.49	59.32	72.83
Nutrient index (NI)	22.85	20.29	39.76	56.52	39.08	67.27	80.07
Cold-water taxa	21.58	19.88	35.91	47.35	33.49	59.32	72.83
Warm-water taxa	75.30	80.12	59.93	41.87	59.59	32.30	21.21
Temperature index (TI)	22.18	19.88	37.59	52.77	36.00	64.73	77.46
nMDS Axis 1	-0.31	-0.27	-0.08	0.07	0.14	0.06	0.08
nMDS Axis 2	-0.03	0.06	-0.01	-0.03	0.01	0.06	0.11

a. *Chiasmolithus edentulus* Subzone (NTp7B)

At G. Nezazat, the *Chiasmolithus edentulus* Subzone (NTp7B) is recorded, which spans the interval from the LO of *Ch. edentulus* to the lowest consistent occurrence (LCtO) of *Sphenolithus primus*. This subzone has a thickness of 3.5 m at G. Nezzazat section. *Chiasmolithus edentulus* occurs in considerable numbers of specimens throughout the Danian/Selandian interval in the study section. It disappears within Zone NP5. The LO of *Chiasmolithus edentulus* was used to directly correlate the Tethys and type area at Zumaia across the D/S boundary.

b. *Sphenolithus primus* Subzone (NTp8A)

This zone includes the biostratigraphic interval from the LCtO of *S. primus* to the LOs of *L. ulii* and *L. billii* at G. Nezzazat section and attains a thickness of about 1 m. *S. primus*, in the first part of its range, is very rare at Site 1262, South Atlantic (Monechi et al. 2013), and it is also rare in the study section. The LO of *S. primus* has been utilized by Varol (1989) to define the base of Zone NTp8 and by Quillévéré et al. (2002) to subdivide Zone NP4 in Subzones NP4a and NP4b.

iii. *Fasciculithus ulii* Subzone (NTp8B)

It defines from the interval from the LO of *Lithoptychius ulii* to the LO of *L. janii*. This subzone has a thickness of about 80 cm, in the study section. The first representatives of *Diantholitha* (*D. alata*, *D. magnolia*) were also observed in this subzone at G. Nezzazat section. On the other hand, *Pontosphaera* sp. first appears at the base of NTp8B at this section.

iv. *Fasciculithus janii* Subzone (NTp8C)

This zone comprises the interval from the *Lithoptychius janii* to the LO of *Fasciculithus tympaniformis* with a thickness of about 1.60 m, in the Nezzazat section. The Genus *Teweius* first occurs within uppermost of NTp8C, and first representative by *Teweiu tovae* of the study section. At El Qrieya section (Egypt), the LO of *L. schmitzii* first occurs within NTp7B (Monechi et al. 2013), and it first occurs at the upper part of NTp8C in our study section.

Fasciculithus tympaniformis Zone (NP5)

The LO of *F. tympaniformis* was used to define the base and *Heliolithus kleinpellii* is used to define the top of Zone

NP5. At Nezzazat section, *F. involutus* and *F. tympaniformis* co-occur at base NP5 Zone (Appendix A). This zone covers the upper part of the Dakhla Fm in the studied section. *Chiasmolithus edentulus* occurs in considerable numbers of specimens throughout the Danian/Selandian interval in the study. It disappears within Zone NP5. The first appearance of *T. eminens* occurs within Zone NP5 in the study section; it is easily recognizable and postdated the LO of *F. tympaniformis*. This observation is marked also in many sections as in site 384 and 1262 in the North Ocean (Westerhold et al. 2008), and also at Duwi section, Quseir area (Farouk and Faris 2013). At G. Nezzazat section, *F. involutus* and *F. tympaniformis* co-occur at the base of NP5. This zone attains a thickness of about 3.5 m (Fig. 2).

Heliolithus kleinpellii Zone (NP6)

The LO of *Heliolithus kleinpellii* is used to define the base of Zones NP6 and CP5 (Martini 1971; Okada and Bukry, 1980). In this study, The LOs of *H. kleinpellii* and *Discoaster mohleri* are used to determine the lower and upper limits of Zone NP6 respectively. This zone spans most of the uppermost part of the Dakhla Fm and its thickness is about 1.75 m (Fig. 2).

Discoaster mohleri Zone (NP7/8)

This zone defines as the interval from the LO of *D. mohleri* to the LO of *D. multiradiatus* as suggested by Romein (1979). The Zone NP/8 corresponds to the terminal part of Dakhla Fm, beside the whole of the Tarawan Fm of the studied section. At G. Nezzazat section, the LO of *Sphenolithus anarrhopus* emulates the base of Zone NP7/8. *Sphenolithus anarrhopus* found near the bottom of Zone NP6 (Romein 1979). At Nezzazat section, *L. bitectus* and *F. alanii* first occurred within Zone NP7/8.

Nannofossil paleoecology

Dominated taxa

Forty-eight nannofossil species were identified from the 41 samples that spanning the Danian-Thanetian in the studied section. Fortunately, the preservation quality in general is good (Fig. 3). In addition, few species have wide stratigraphic ranges, while most of them are age diagnostic and have limited ranges (Fig. 4). Moreover, most of them are well-known paleoclimatic indicators. Therefore, there distribution pattern can be used as a pleoenvironmental indicators. The pre-Danian (LDE) is dominated by *Zeugrhabdotus sigmoides* (a cool-water indicator) and *Neochiastozygus modestus* (Fig. 4). The post-Danian interval (NTp8B) is dominated by *Coccolithus pelagicus* and *Ericsonia subpertusa* reaching 11.9% and 12.7% respectively (Fig. 4; Appendix A). *Cruciplacolithus* and *Neochiastozygus* spp. show low abundance during this interval (Fig. 5).

During the rest of the Selandian, *Lithoptychius* was dominated but *Fasciculithus* became scarce (Fig. 5). In addition, *Neochiastozygus* and *Cruciplacolithus* increased again and reached the pre-LDE abundances (Fig. 5), which indicated the return to the stable conditions. Before the onset of the Selandian-Thanetian boundary, a marked shift in the nannofossil species was observed (probably the onset of the ELPE). *Fasciculithus* increased significantly, while marker Danian-Selandian genera (e.g., *Lithoptychius Neochiastozygus*, *Chiasmolithus*, and *Cruciplacolithus*) decreased dramatically (Fig. 5).

Nannofossil assemblages

The dendrogram resulting from clustering shows that the samples belonging to Thanetian can be clustered together away from proceeding samples (Fig. 6). The post-Danian samples (NTp8B) were clustered also together but with more similarities to both processed and succeeded samples (Fig. 6). These patterns can indicate no marked faunal changes in the Danian-Selandian. To test for significant differences among of these assemblages, the non-parametric PerMANOVA test based on Bray–Curtis similarity coefficient was implemented. The results indicated no significant difference among most of the assemblages except for middle Selandian assemblage (NT p8C), which significantly differs from the underlaying (NT p8B) and the overlaying assemblage (NP5; Table 1).

To characterize the differences among the proposed assemblages further, ordination technique was used. The 2D nMDS plot shows a clear distinction among the nannofossil assemblages grouped based on their stratigraphic positions (zones and subzones). The samples and assemblages were scattered along nMDS Axis 1, where younger samples plotted to the left with negative values, while older samples plotted to the right with positive values (Fig. 7). 2D-NMDS plot shows no overlap among the assemblages (Fig. 7). This can indicate a marked faunal change not only between ages but also between nannofossil biozones. The change of the dominated species is interpreted herein to be controlled mainly by the environmental changes.

To understand the role of the biotic variables behind the 2D-nMDS plot, a series of RMA linear regression models were conducted. The results indicated no significant correlation ($R^2 = 0.20$; p level $= 0.001$) between the biodiversity (Shannon index) and nMDS Axis 1 (Fig. 8). A significant correlation ($R^2 = 0.23$; p level $= 0.001$)) was found between the Dominance index and nMDS Axis 2. However, most of the samples have the same range on the 2D plot (Fig. 7), indicating that the role of biodiversity is of minor

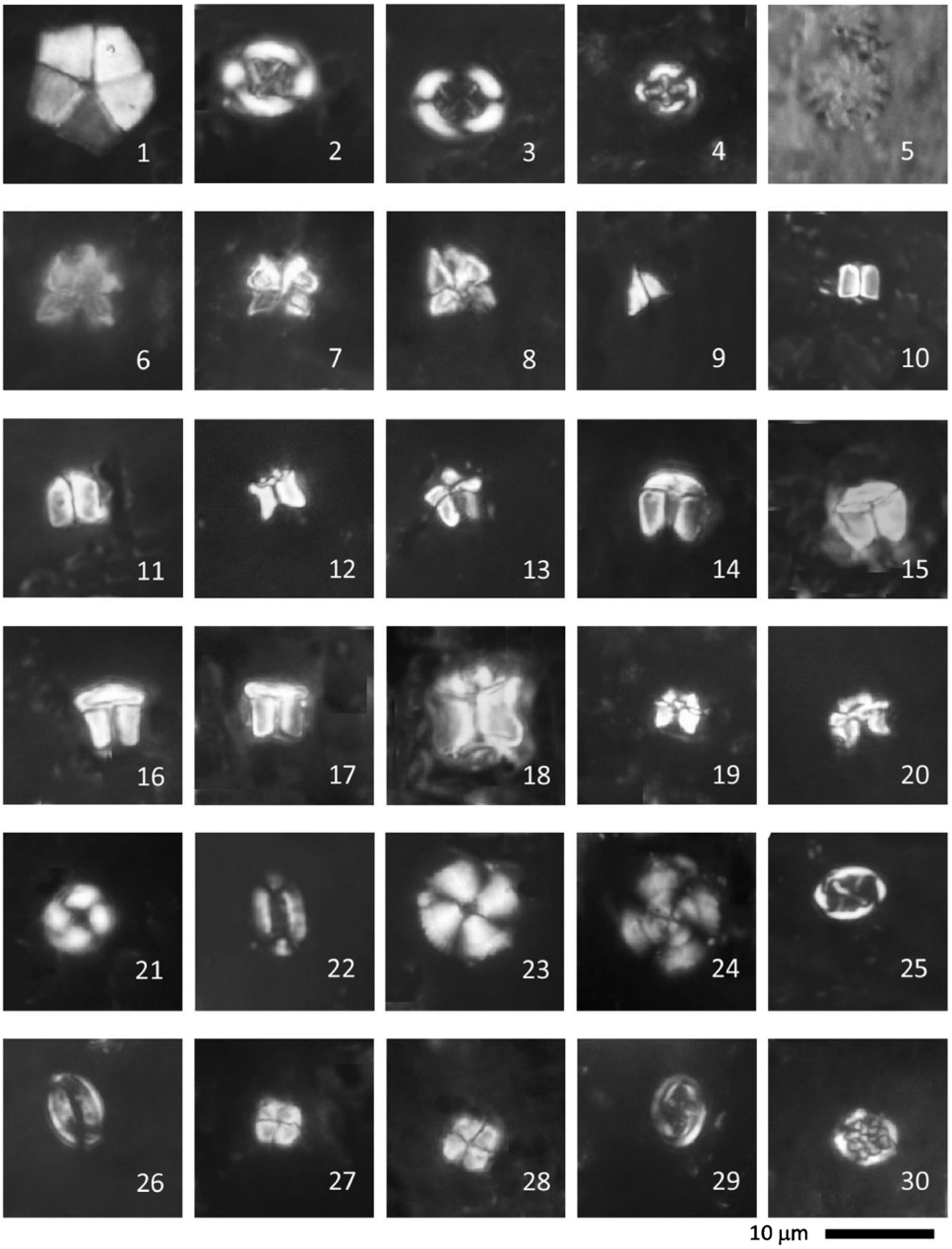

Fig. 3 Dominated nannofossils species in EAB basin; A: *Braarudosphaera bigelowii* (Gran and Braarud, 1935) Deflandre (1947), sample 17. B, C: *Chiasmolithus bidens* (Bramlette and Sullivan, 1961), sample 37. D: *Cruciplacolithus tenuis* (Stradner, 1961) Hay and Mohler in Hay et al. (1967), sample 18. E: *Discoaster mohleri* Bukry and Percival (1971), sample 38. F, G: *Diantholitha magnolia* Aubry and Rodriguez (2011), sample 19. H: *Diantholitha alata* Aubry and Rodriguez (2011), sample 24. I: *Fasciculithus alanii* Perch-Nielsen (1971), sample 40. J: *Fasciculithus involutus* Bramlette and Sullivan (1961), sample 37. K: *Fasciculithus tympaniformis* Hay and Mohler in Hay et al. (1967), sample 38. L: *Lithoptychius billii* (Perch-Nielsen, 1971) Aubry in Aubry et al. (2011), sample 11. M: *Lithoptychius collaris* Aubry and Rodriguez (2011), sample 19. N, O: *Lithoptychius pileatus* Bukry (1973) Aubry (2011), sample 34. P: *Lithoptychius janii* (Perch-Nielsen, 1971) Aubry in Aubry et al. (2011), sample 23. Q: *Lithoptychius stegastus* Aubry and Bord (2011), sample 10. R: *Lithoptychius ulii* (Perch-Nielsen 1971b) Aubry (2011), sample 24. S: *Lithoptychius felis* Aubry and Bord (2011), sample 14. T: *Lithoptychius schmitzii* Monechi et al. (2013), sample 14. U: *Ericsonia subpertusa* Hay and Mohler (1967), sample 3. V: *Ellipsolithus macellus* (Bramlette and Sullivan, 1961), sample 1. 23: *Heliolithus cantabriae* Perch-Nielsen (1971), sample 37. X: *Heliolithus kleinpellii* Sullivan (1964), sample 36. Y: *Neochiastozygus perfectus* Perch-Nielsen (1971), sample 29. Z: *Pontosphaera* sp., sample 9. AA, AB: *Sphenolithus primus* Perch-Nielsen (1971), sample 33. AC: *Zeugrhabdotus sigmoides* (Bramlette and Sullivan, 1961) Bown and Young (1997), sample 29. AD: *Thoracosphaera saxea* Stradner (1961), sample 12

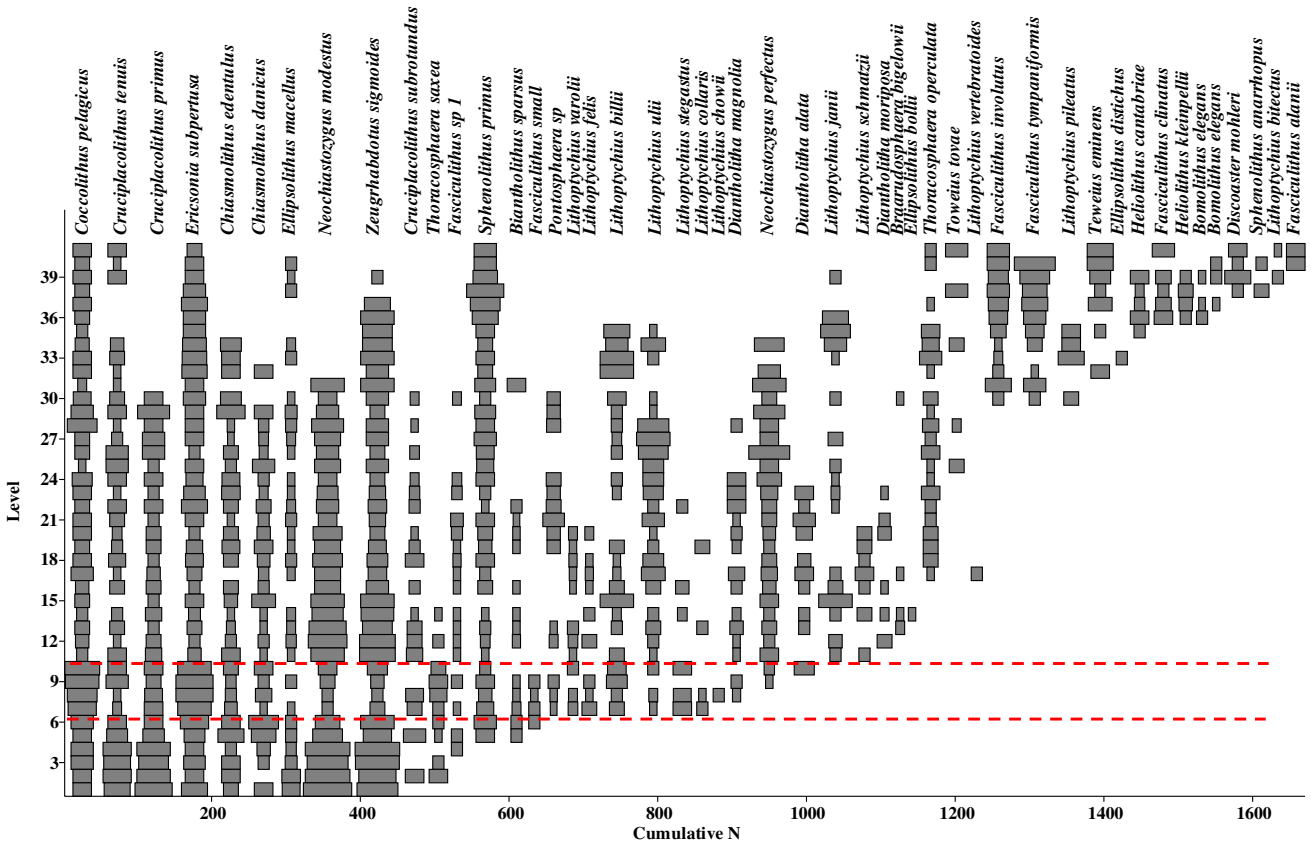

Fig. 4 Vertical distribution of the calcareous nannofossils species in G. Nezzazat. Level: sample number, Cumulative N: the cumulative number of all individuals of all species

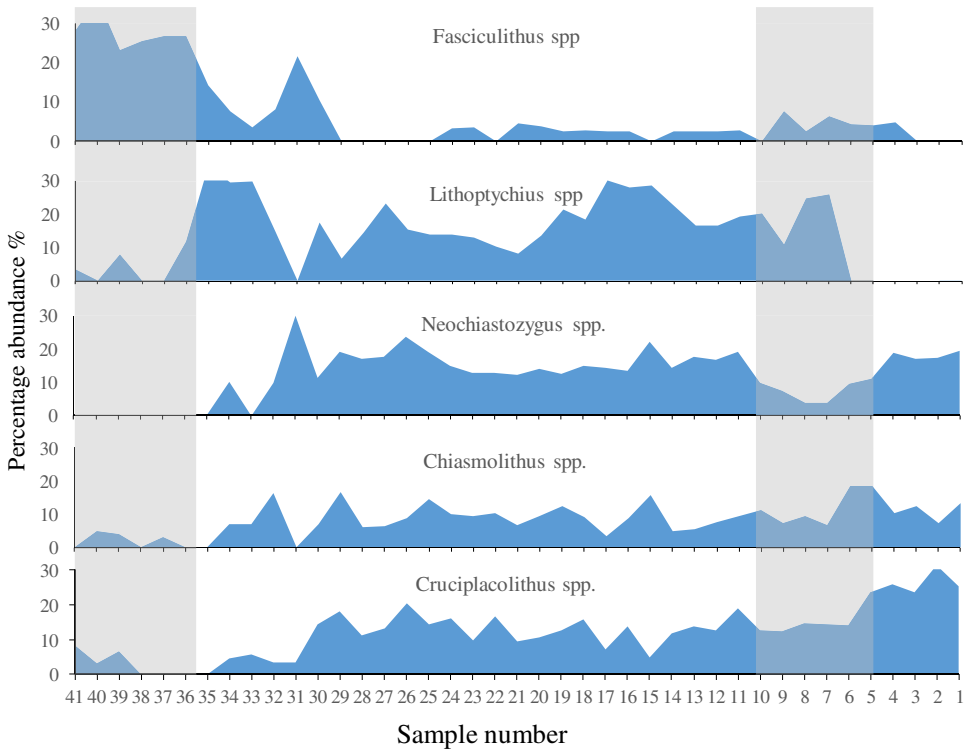

Fig. 5 Percentage abundance of the main nannofossils species in G. Nezzazat

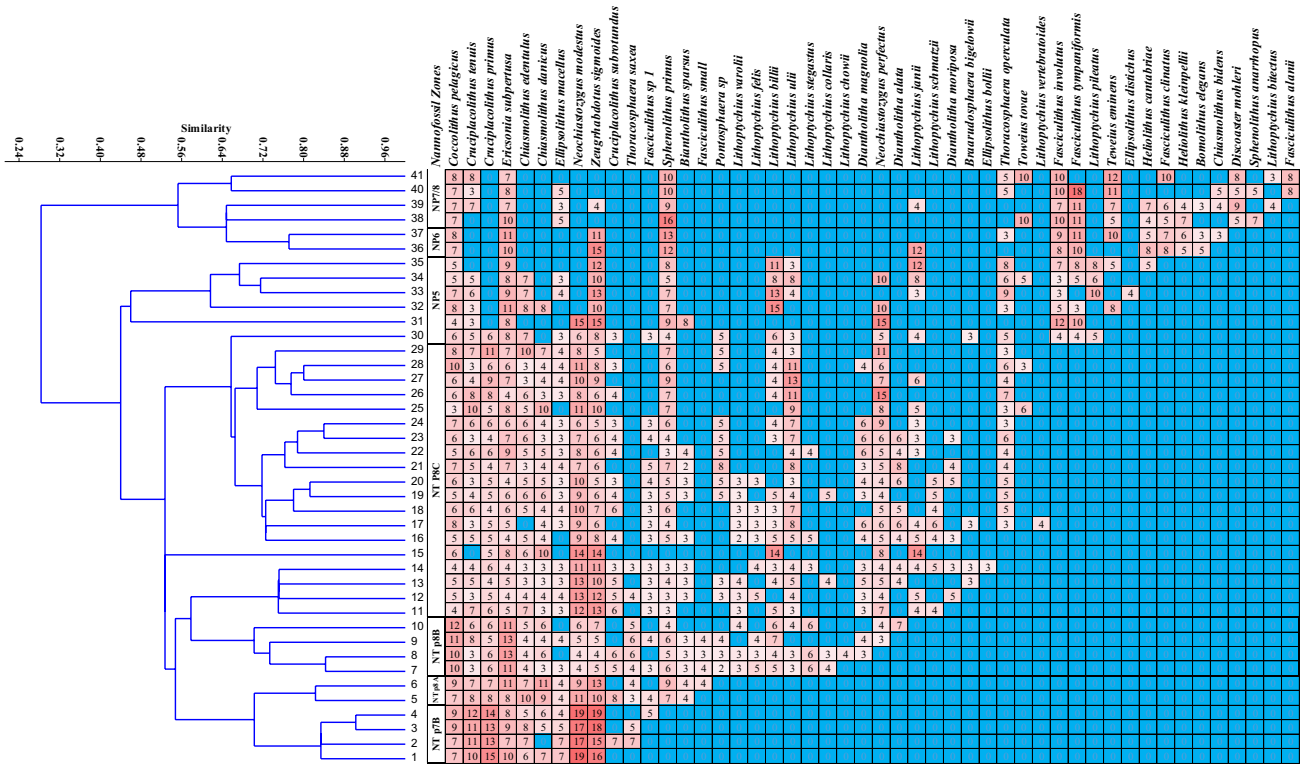

Fig. 6 Bray–Curtis-based, stratigraphic constrained clustering dendrograms (ccc = 0.88) showing the potential assemblages note that Selandian/Thanetian assemblage is well differentiated from proceeding ones

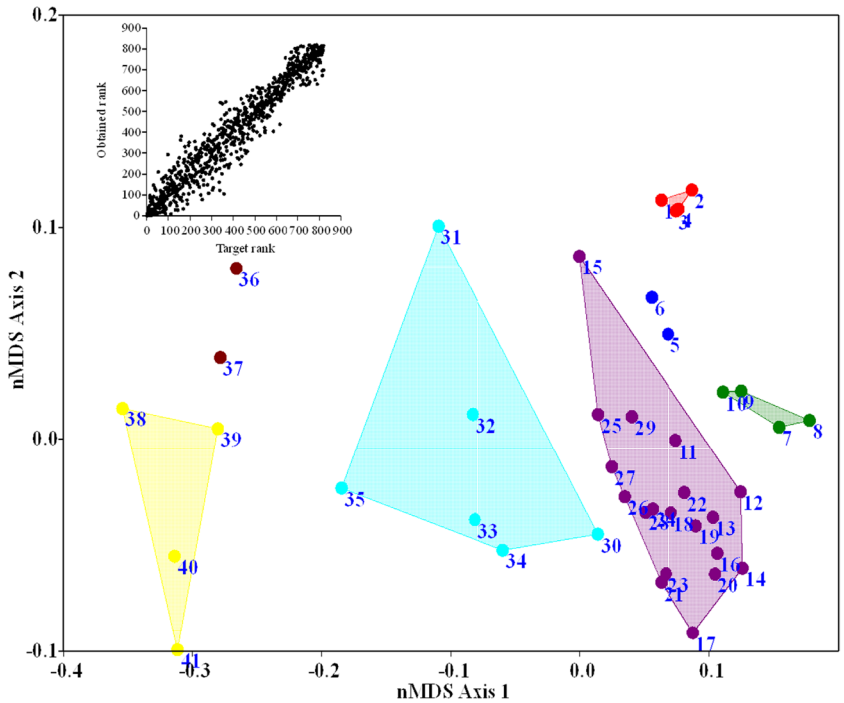

Fig. 7 2D Bray–Curtis-based nMDS plot visualizes the relationship among these assemblages grouped based on nannofossil zones

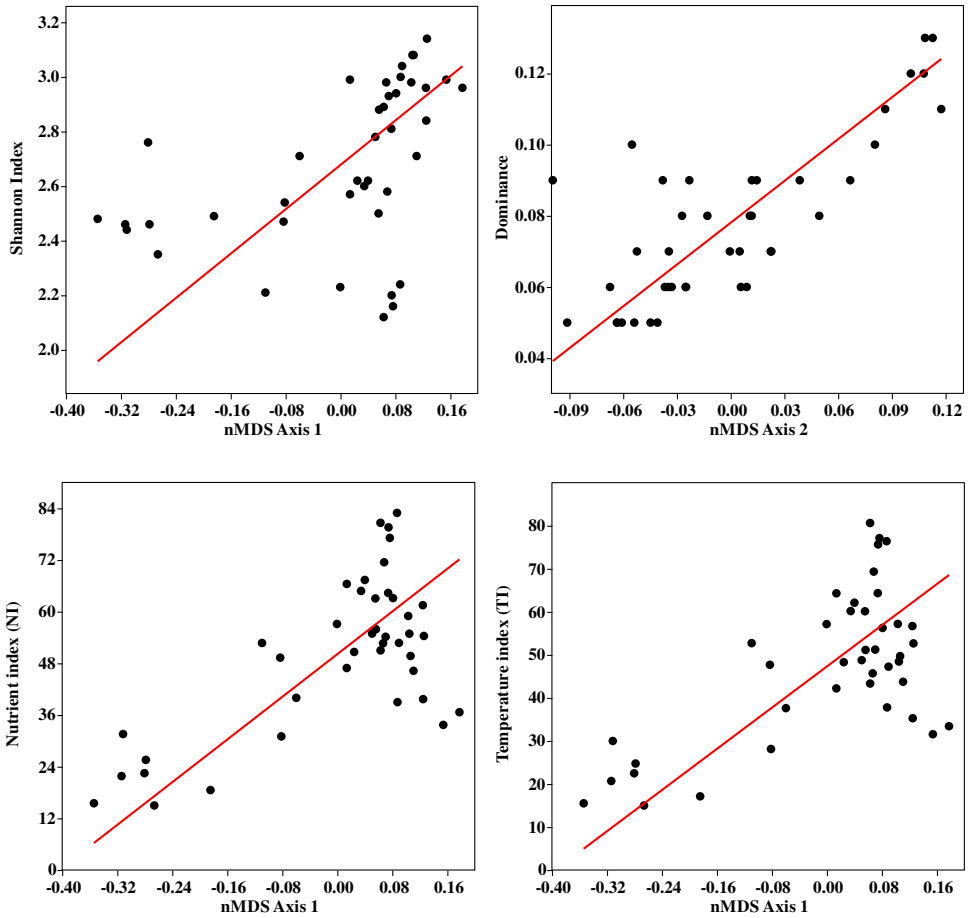

Fig. 8 RMA Linear regression models among the nMDS Axis 1 and Shannon index (A), nMDS Axis 2 and Dominance index (B), nMDS Axis 1 and Nutrient index (C), nMDS Axis 1 and Temperature index (D)

importance. In contrast, string positive correlation was found between nMDS Axis 1 and both of NI and TI ($R^2 = 0.62$; 0.60, respectively; p level = 0.001; Fig. 8), which indicated that temperature and fertility is a major factor differentiated among the studied nannofossil assemblages.

Nannofossil indices

The percentage of meso-eutrophic taxa decreases significantly at the LDE but retained higher values again from the sample 11 (NTp8B) onward (Fig. 9). The meso-eutrophic taxa dropped again dramatically prior to the S/T transition (NPZ 6) and remained low to the topmost parts of the section (Fig. 9). The same pattern is also clear in other indices. The cool-water taxa decreased significantly at the LDE and again at the ELPE (Fig. 9). The Diversity (Shannon and Evenness) was very low prior to the LDE but increased slightly after the LDE and remains slightly stable in the Selandian but decreased again slightly at the S/T transition. Similarly, Dominance was very high at the LDE and decreased slightly afterward but increased again during the S/T transition (Fig. 9). These patterns of changes in the nannofossils reflected clearly in the two nMDS Axis 1 and 2, which indicate that they represent the environmental changes in the nannofossil distribution very well.

Discussion

Despite scarce investigations, paleoclimatic reconstructions of the relatively cool mid-Paleocene (62–58 Ma) interval can provide a better insight of how the transition from greenhouse towards hothouse affected the ecosystem. Due to the low sea level, sedimentary archives that capture this time interval are scarce (Westerhold et al. 2008; De Storme et al. 2014). Herein, a general cooling climate during the mid-Paleocene was dissected by two hyperthermal events: the Latest Danian Event (LDE) and the Early Late Paleocene Event (ELPE).

Nannofossil bioevents

Based on the nannofossil distribution, ordination and clustering, and nannofossil indices, two main bioevents can be clearly indicated. The first bioevent, the LDE, was abrupt at the D/S boundary and lasted throughout the NTp8B subzone. The nannofossils in this event are mainly of

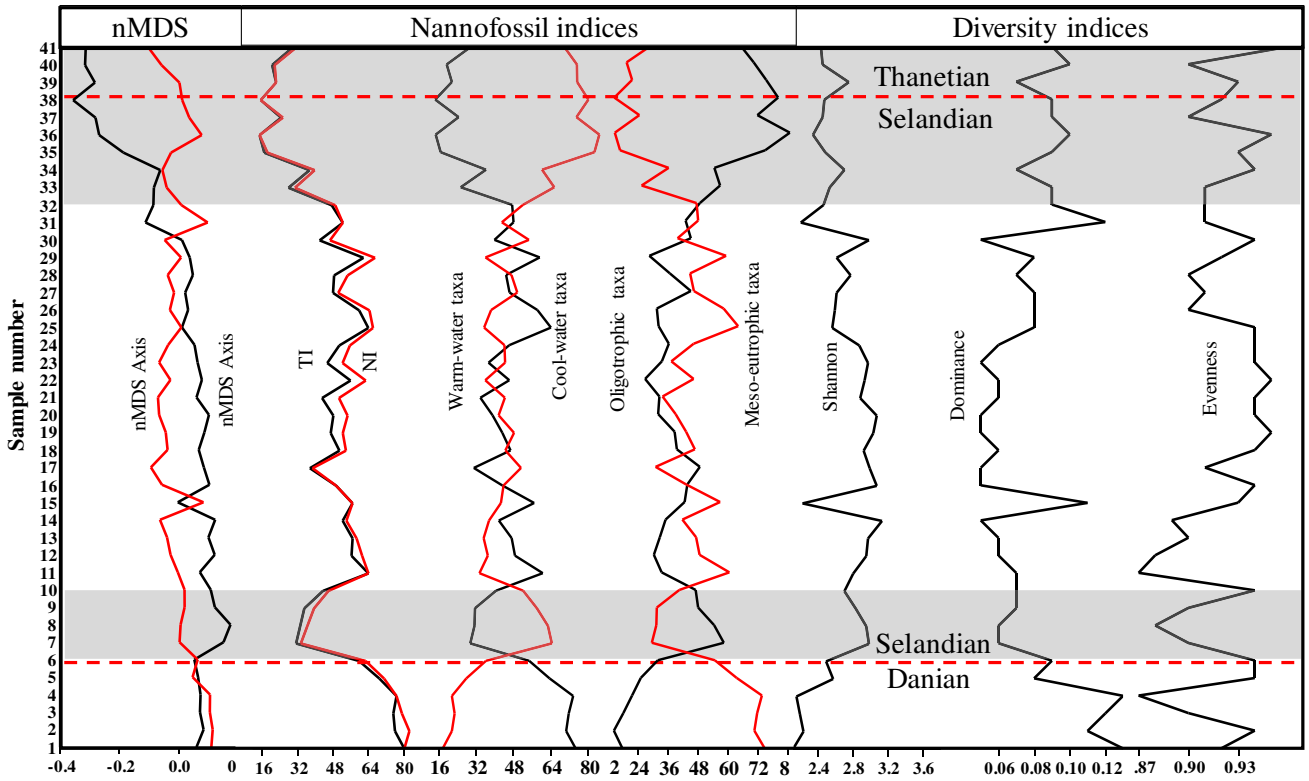

Fig. 9 Vertical trend in nMDS Axis 1 and 2, Temperature index (TI), Nutrient index (NI), and Diversity indices. Marked increases in temperature and decrease nutrients at both LDE and ELBE are obvious (shaded), while Diversity fluctuated throughout the study section

warm-oligotrophic environments and are highly distinct from the proceeded ones (Fig. 9). The pre-LDE nannofossils with cooler and eutrophic climatic conditions prevailed in both pre-event and post-event assemblages. The warmer and oligotrophic conditions initiated again prior to the S/T boundary (ELPE). The climatic changes during ELPE were gradual and continued after the S/T boundary to the end of the section (NP7/8; Fig. 9). The diversity was not obviously affected during both events. The very low diversity before the LDE can be attributed to pronounced sea-level fall. Significant differences were found between the event assemblages and the background ones (p level < 0.001; Fig. 10). The main differences are in TI and NI. In contrast, no significant difference was found based on diversity (Shannon index; Fig. 10).

The two minor hyperthermal events proceeded the Paleocene-Eocene thermal maximum (PETM). This ~ 2–3 °C transient warming event associated with a 0.5–2% carbon isotope excursion "CIE" at the LDE has been identified globally in the Pacific Ocean, Atlantic Ocean, Northern Tethys, and Southern Tethyan shelf (Westerhold et al. 2008, 2011; Dinarès-Turell et al. 2012; Sprong et al. 2013). Dinarès-Turell et al. (2012) linked the LDE event to volcanism in the North Atlantic Igneous Province.

Latest Danian Event

In Egypt, the LDE is placed at the base of an organic-rich dark bed (formerly thought to mark the D/S boundary) that contains a characteristic benthic foraminiferal assemblage with common *Neoeponides duwi* (Speijer and Schmitz, 1998, Speijer 2003; Guasti et al. 2005), a shallow-water (inner neritic) species. This assemblage, however, has not been recognized in other neritic sections from the Southern Tethyan margin (Guasti et al. 2006).

Kasem et al. (2022) found no marked changes in calcareous nannofossil assemblages and argued this to the dominance of oligotrophic warm-water conditions throughout the Paleocene. They have found that Danian-Selandian transition marks a decrease in warm and oligotrophic conditions that persisted along the Selandian Stage. The Selandian-Thanetian transition shows an increase in warm and oligotrophic conditions. Moreover, they attributed the abrupt decrease in calcareous nannofossils in the Selandian and Thanetian to carbonate dissolution and not the paleotemperature and/or paleofertility.

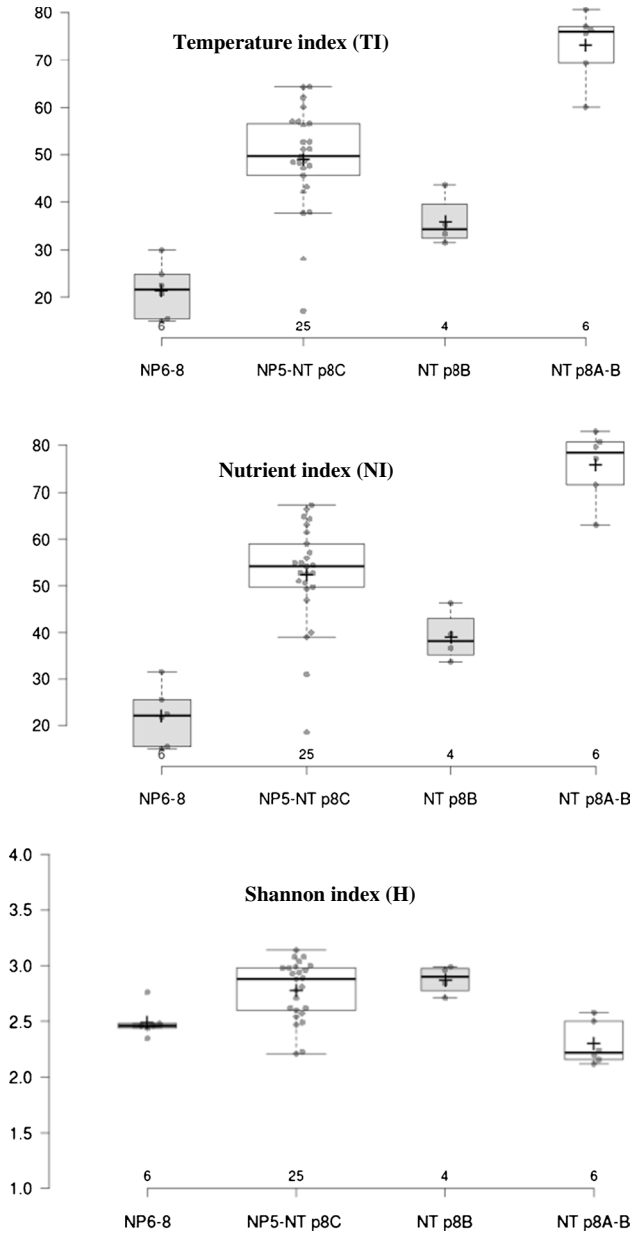

Fig. 10 Box plots show a significant difference in TI and NI between hyperthermal events and background conditions. No significant difference was found in biodiversity

Early Late Paleocene Event

Another hyperthermal event was also recorded in the western Tethys at the Selandian-Thanetian transition with marked environmental perturbation (Egypt, Tunisia, Morocco, Spain, and Italy), Central Pacific, and New Zealand (Coccioni et al. 2019). In Egypt, the S/T boundary is placed at the Maximum Flooding Surface (MFS) above the Mid-Paleocene Biotic Event (MPBE; Hewaidy et al. 2019), where the highest planktonic/benthonic (P/B) ratio (90%) was recorded (see also Shahzad et al. 2023). Pujalte et al. (2014) concluded that the ELPE represents a long period of stressed oceanic conditions. Contreras et al. (2014) based on marine pollen record (ODP Site 1172, East Tasman Plateau) indicated that cool-temperate forests prevailed at the middle/late Palaeocene transition interval (~ 59.5 to ~ 59.0 Ma). Hollis et al. (2022) indicated a general CO2 decline and climatic cooling in the southwest Pacific during the Late Paleocene. They argued the absence of "hypothermal" events to erosion and carbonate dissolution in deep-sea sediment.

Environmental controls

During the Selandian, marine transgressions were observed in many localities of Egypt (Lüning et al. 1998; Farouk and Faris 2013). They can be linked with the global hyperthermal at ~61.6 Ma (LDE). Berggren et al. (2012) noted that the Selandian/Thanetian boundary is located within the middle part of the Tarawan Chalk Formation. They added that P/B ratio was dramatically decreased, which may point to forced regression. Farouk and Faris (2013) indicated that this boundary is characterized by forced regression, with marked changes in sedimentary facies (from the Dakhla Shale to the Tarawan Chalk the upper part of the P4 foraminiferal zone).

The Genus *Chiasmolithus* is well known as a cool- to cold-water taxon (Wei and Wise 1990; Firth and Wise 1992; Bralower 2002). In our study, *Fasciculithus* and *Sphenolithu* are closely associated with *Discoaster* and scarce in this interval, so they were thought to have adapted to warm-water, oligotrophic conditions (Haq and Lohmann, 1976; Wei and Wise 1990). As a result, the conditions in this interval reverted to those conditions that prevailed in the pre-event interval with an abundance of *Toweius* spp. (Figs. 4 and 5). From the above-mentioned information, we can conclude the paleoclimate in the present section as follows: In the pre-event and post-event assemblages, cooler climatic conditions prevailed in the studied area, as evidenced by sharp increases in the abundance of *Z. sigmoides*, a cool climate index (Appendix A).

Obaidalla et al. (2009) indicated a shallowing from the outer neritic environment for the main Danian and Selandian sediments to a middle neritic setting at the D/S boundary (Qreiya Bed). The general decrease in temperature may be related to a dissolution coinciding with the Mid-Paleocene Biotic Event (MPBE) or Early Latest Paleocene Event (ELPE) (Bralower 2002; Petrizzo, 2005; Bernaola et al. 2007; Westerhold et al. 2011). Guasti et al. (2006) argued the increase in paleoproductivity to the shallowing from the Danian to the Selandian, which was associated with increasing terrigenous input. Westerhold et al. (2011) indicated that

productivity would increase in the climate warming stage as a consequence of intensified precipitation and terrestrial input.

In the Southern Tethys (Egypt and Tunisia), a change from a deep oligotrophic to a shallower eutrophic regime was recorded based on nannofossils that have been documented (Guasti et al. 2006; Sprong et al. 2013). The sea-level fall was also recorded at other localities (e.g., the North Sea). Alegret et al. (2016) indicated also increasing nutrients at the LDE in Spain (Caravaca) but without marked changes in the sea level. Devleeschouwer et al. (2016) indicated dysoxic to anoxic conditions at the base of the selandian. Speijer (2003) argued the perturbation at the S/T to the sea-level rise, where organic carbon-rich laminated sediments were accumulated at dysoxic seafloor about 60.5 Ma, which may be linked to global warming events. Devleeschouwer et al. (2016) indicated increasing terrigenous input at the base of the Selandian due to eustatic sea-level shallowing. The shallowing at the D/S boundary was also earlier indicated (Obaidalla et al. 2009). They also found that the warm condition at the D/S boundary interrupts a general background cooling.

Diversity dynamics

Based on the high-resolution biostratigraphic scheme, we refute the dissolution or incompleteness of the study section. The general low diversity and high dominance at both transitions (i.e., D/S and S/T) suggest environmental stress. Speijer (2003) indicates that The S/T transition was a time of ecological stress for both calcareous nannofossils and foraminifera, suggesting marked environmental perturbation in the ocean chemistry. Coccioni et al. (2019) have recorded long and short (~350Kyr) events in the western Tethys (Gubbio, Italy) with marked environmental deterioration during the middle-early late Paleocene.

Intra-basinal correlation

The zonal boundaries were accurately determined by the nannofossil bioevents, which provide an optimal stratigraphic resolution (see Abdelhady et al. 2019a, b, 2018). Therefore, climatic reconstruction can be inter-regionally correlated. The nannofossil bioevents that well identified in the present study (G. Nezzazat section, WC Sinai, Egypt)

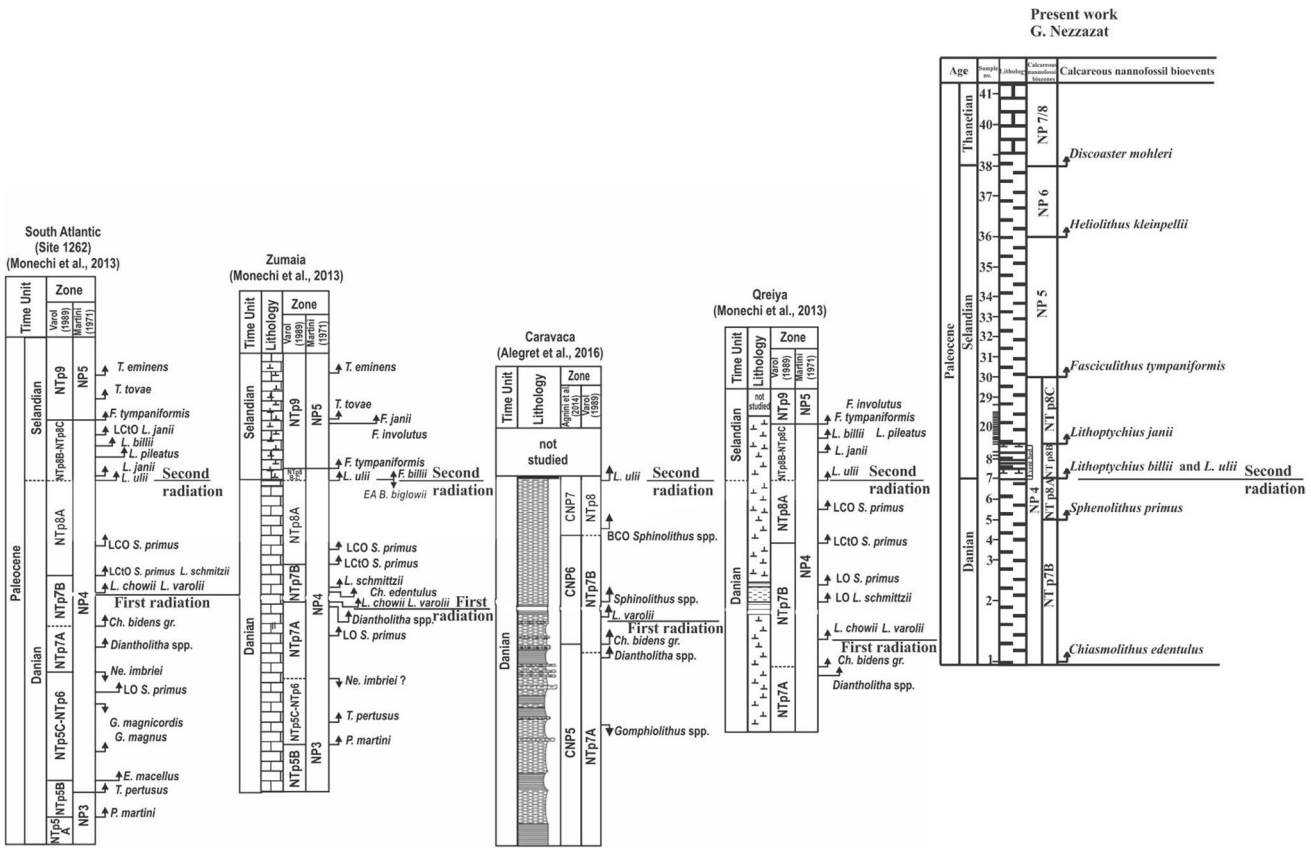

Fig. 11 Stratigraphic correlation of the middle Paleocene bioevents in G. Nezzazat and South Atlantic (Site 1262), Zumaia, and Qreiya sections (Monechi et al. 2013) in addition to Caravaca section (Alegret et al. 2016). Not to scale

allows accurate correlation between the D/S boundary at the type area (Zumaia section), with the bioevents of South Atlantic (Site 1262), Qreiya section, and Caravaca section (Fig. 11). The main bioevents and correlation of the current study can be summarized in the following: (1) The biozonation of Varol (1989) allows a more precise division of the studied interval and direct correlation with the Tethys area. (2) The LO of *Chiasmolithus edentulus* is the best calcareous nannofossil bioevent that can be used to correlate the Tethys and the type area across the D/S boundary (Varol 1989). (3) The LCO of *Sphenolithus primus* could be utilized for regional biostratigraphic correlations. (4) From the present study, it appears that the best event for global, marine correlation is the Second Radiation of LO of *Lithoptychius ulii* (Fig. 4).

In the North Sea, this boundary can be traced between zones NP4 and NP5, and within the planktic foraminifera P3 Biozone (Clemmensen and Thomes (2005). The "Neoduwi event" is a term of brief biotic and sedimentary event within the D/S boundary in Egypt and Jordan, and is located within basal Zone P3b, towards the top of Zone NP4 (Guasti et al. 2005). Guasti et al. (2006) postulated a hiatus at the D/S boundary at the P3a/P3b subzonal boundary within the nannofossil Zone NP4 that aligns with a unique glauconitic marl bed (50 cm thick) in Tunisia. At Wadi Tarfa, Egypt's northeastern Desert, this boundary was drawn at the base of P3b, which locates at the base of organic-rich phosphatic shale (Obaidalla 2006). Obaidalla et al. (2009) delineated the D/S boundary at Qreiya section (Egypt) based on several analyses (geochemical, mineralogical, and planktic foraminifera) within the upper part of P3b Subzone and at the base of four alternative black and brown organic-rich phosphatic layers of about 30 cm thick. Sprong et al. (2006) studied the paleoenvironment of the D/S boundary at Qreiya section (Eastern Desert, Egypt) and traced this boundary at the P3a/P3b boundary and within the nannofossil Zone NP4. The D/S boundary at the Qreiya section is situated using nannofossils at the base of NTp8C, which is delineated by the LO of *Lithoptychius janii* (Youssef 2003).

At the Zumaya section (Spain), the D/S boundary was placed between the Danian limestone and marls of Itzurun Formation and defined at the level of end acme of *Braarudosphaera bigelowii* (Bernaola et al. 2009; Schmitz et al. 2011). The end acme of *B. bigelowii* cannot be detected in subtropical and tropical areas (Bernaola et al. 2009), and the D/S boundary cannot be located by it the present study, but on the basis of calcareous nannofossils the Second Radiation of *Fasciculithus* taxa (LO of *Lithoptychius ulii*, base NTp8B) was used for approximation the base of the Selandian in the study section (G. Nezzazat). At Zumaia, the onset of a second diversification of the genera *Fasciculithus* represented by LOs of *Lithoptychius janii* and *Lithoptychius ulii* characterizes the event. At the study section, the calcareous nannofossil assemblage in the Selandian Stage is dominated by the same species that prevail in the Danian Stage beside the LOs of *L. ulii*, *L. billii*, and *Pontosphaera* sp. (base NTp8B; Fig. 11).

Conclusions

Quantitative analyses of the nannofossils of the G. Nezzazat section (west central Sinai) was done to reconstruct the paleoclimate (surface water temperature and fertility) during the latest Danian–early Thanetian interval (ca. 5.5 My) in the southwestern Tethys (Egypt). We can conclude the following:

- The study sequence belongs to the nannofossil biozones *Ellipsolithus macellus* (NP4). *Fasciculithus tympaniformis* (NP5), *Heliolithus kleinpellii* (NP6), and *Discoaster mohleri* (NP7/8). The Danian/Selandian boundary lies at the base of NTp8B (Second Radiation of *Fasciculithus*), without a significant turnover of nannofossil assemblages and no dissolution, and thus, the Nezzazat section represents a continuous record of the D/S transition. The Selandian/Thanetian boundary can be traced between the nannofossil zones NP6 and NP7/8 (LO of D. *mohleri*) in the study section and can be placed in the uppermost part of the Dakhla Formation.
- In contrast to most recent investigations, marked changes in the nannofossil community structure characterize both Paleocene hyperthermal. However, no marked biodiversity changes were found.
- The change in the dominant species is interpreted to be controlled mainly by environmental conditions instead of diagenetic dissolution.
- The very low diversity prior to the D/S was attributed mainly to sea-level changes, where the LDE is placed at the sequence boundary (forced regression). In contrast, the S/T boundary represents the maximum flooding setting.
- Both pre-event and post-event assemblages in the study section are indicators of eutrophic cooler climatic conditions, which are dissected by short-lived hyperthermal events at the D/S and the S/T transitions with an oligotrophic regime.

Supplementary Information The online version contains supplementary material available at https://doi.org/10.1007/s12517-023-11566-z.

Acknowledgements Anonymous reviewers are highly acknowledged for their constructive comments.

Funding This research was funded by Researchers Supporting Project number (RSP2023R455), King Saud University, Riyadh, Saudi Arabia.

Data Availability All data used in this study are provided as online supplementary material.

Declarations

Conflict of interest The authors declare no competing interests.

References

Abdelhady AA, Seuss E-D, Obaidalla NH, Mahfouz AK, Hussien SAA (2018) The Unitary Association method in biochronology and its potential stratigraphic resolving power: a case study from Paleocene-Eocene strata of southern Egypt. Geobios 51(4):259–268

Abdelhady AA, Kassab W, Aly MF (2019a) Shoal environment as a biodiversity hotspot: a case from the Barremian-Albian strata of Gabal Lagama (North Sinai, Egypt). J African Earth Sci 160:103643. https://doi.org/10.1016/j.jafrearsci.2019.103643

Abdelhady AA, Seussb B, Hassan H (2019b). Stratigraphic ranking of selected invertebrate fossils: a quantitative approach at different temporal and geographic scales. Palaeontologia Electronica 22.2.51A 1–17. https://doi.org/10.26879/912

Agnini C, Fornaciari E, Raffi I, Rio D, Röhl U, Westerhold T (2007) High-resolution nannofossil biochronology of middle Paleocene to early Eocene at ODP Site 1262: implications for calcareous nannoplankton evolution. Mar Micropaleontol 64:215–248

Alegret L, Ortiz S, Arreguín-Rodríguez GJ, Monechi S, Millan I, Molina E (2016) Microfossil turnover across the uppermost Danian at Caravaca, Spain: paleoenvironmental inferences and identification of the latest Danian event. Palaeogeogr Palaeoclimatol Palaeoecol 463:45–59

Ali MY (2009) High resolution calcareous nannofossil biostratigraphy and paleoecology across the Latest Danian Event (LDE) in central Eastern Desert. Egypt Marine Micropaleontol 72(3–4):111–128

Anthonissen DE, Ogg JG (2012) Cenozoic and Cretaceous biochronology of planktonic foraminifera and calcareous nannofossils. In The geologic time scale (pp. 1083–1127). Elsevier

Arenillas I, Molina E, Ortiz S, Schmitz B (2008) Foraminiferal and Δ13C isotopic event-stratigraphy across the Danian-Selandian transition at Zumaya (northern Spain): chronostratigraphic implications. Terra Nova 20:38–44

Arreguín-Rodríguez GJ, Alegret L, Thomas E (2016) Late Paleocene-middle Eocene benthic foraminifera on a Pacific seamount (Allison Guyot, ODP Site 865): Greenhouse climate and superimposed hyperthermal events.". Paleoceanography 31(3):346–364

Awad GH, Ghobrial MG (1965) Zonal stratigraphy of Kharga Oasis. Ann Geol Surv Egypt 34:1–77

Bassiouni MA, Faris M, Sharaby S (1991) Late Maastrichtian and Paleocene calcareous nannofossils from Ain Dabadib section: NW Kharga Oasis. Qatar University Science Bulletin Journal 11:357–375

Berggren WA, Alegret L, Aubry MP, Cramer B, Dupuis C, Goolaerts S, Kent DV, King C, O'B Knox R, Obaidalla N, Ortiz S (2012). The Dababiya corehole, upper Nile valley, Egypt: preliminary results

Bernaola G, Baceta JI, Orue-Etxebarria X, Alegret L, Martín-Rubio M, Arostegui J, Dinarès-Turell J (2007) Evidence of an abrupt environmental disruption during the mid-Paleocene biotic event (Zumaia section, western Pyrenees). Geol Soc Am Bull 119(7–8):785–795

Bernaola G, Martín-Rubio M, Baceta JI (2009) New high resolution calcareous nannofossil analysis across the Danian-Selandian transition at the Zumaia section: comparisons with South Tethys and Danish sections. Geol Acta 7(1–2):79–92

Bornemann A, Schulte P, Sprong J, Steurbaut E, Youssef M, Speijer RP (2009) Latest Danian carbon isotope anomaly and associated environmental change in the southern Tethys (Nile Basin, Egypt). J Geol Soc 166(6):1135–1142

Boucot AJ, Chen X, Scotese CR (2013) Phanerozoic paleoclimate: an atlas of lithologic indicators of climate, SEPM Concepts in Sedimentology and Paleontology, (Digital Version), No. 11, 478 ISBN 978–1–56576–281–7, October 2013 Society for Sedimentary Geology, Tulsa, OK

Bralower TJ (2002) Evidence of surface water oligotrophy during the Paleocene-Eocene thermal maximum: nannofossil assemblage data from ocean drilling program Site 690, Maud rise. Weddell Sea Paleoceanography 17(2):13–21

Bralower TJ, Silva IP, Malone MJ (2005) Leg 198 synthesis: a remarkable 120-my record of climate and oceanography from Shatsky Rise, northwest Pacific Ocean. In Proceedings of the Ocean Drilling Program: Scientific Results (Vol. 198). Texas A & M University

Clarcke KR (1993) Nonparametric multivariate analyses of changes in community structure. Austral Ecol 18(1):117–143

Clark WB, Watkins DK (2020) A quantitative analysis of calcareous nannofossils across a late oligocene paleolatitudinal transect of the North Atlantic Ocean. Mar Micropaleontol 158:101892

Clemmensen A, Thomsen E (2005) Palaeoenvironmental changes across the Danian-Selandian boundary in the North Sea Basin. Palaeogeogr Palaeoclimatol Palaeoecol 219(3–4):351–394

Coccioni R, Frontalini F, Catanzariti R, Jovane L, Rodelli D, Rodrigues IM, Savian JF, Giorgioni M, Galbrun B (2019) Paleoenvironmental signature of the selandian-thanetian transition event (STTE) and early late paleocene event (ELPE) in the Contessa Road section (western Neo-Tethys). Palaeogeogr Palaeoclimatol Palaeoecol 523:62–77

Contreras L, Pross J, Bijl PK, O'Hara RB, Raine JI, Sluijs A, Brinkhuis H (2014) Southern high-latitude terrestrial climate change during the Palaeocene-Eocene derived from a marine pollen record (ODP Site 1172, East Tasman Plateau). Climate of the past 10(4):1401–1420

Devleeschouwer X, Wouters S, Riquier L, Yans J, Storme JY, Steurbaut E (2016). A climatic change at the Danian/Selandian boundary: increasing weathering fluxes. GB2016, 236

De Storme N, Geelen D (2014) The impact of environmental stress on male reproductive development in plants: biological processes and molecular mechanisms. Plant Cell Environ 37(1):1–18

Dinarès-Turell J, Pujalte V, Stoykova K, Baceta JI, Ivanov M (2012) The Palaeocene "top chron C27n" transient greenhouse episode: evidence from marine pelagic Atlantic and peri-Tethyan sections. Terra Nova 24(6):477–486

Elewa AMT, Abdelhady AA (2020a) Paleoecology of the middle Eocene ostracods of Egypt. J African Earth Sci 162:103678. https://doi.org/10.1016/j.jafrearsci.2020.103780

Elewa AMT, Abdelhady AA (2020b) Past, present, and future mass extinctions. J African Earth Sci 164:103780. https://doi.org/10.1016/j.jafrearsci.2019.103678

Faris M (1985) Stratigraphy of the Late Cretaceous/Early Tertiary sediments in Ghanima and Ain Amur sections, Kharga area. Egypt Newsletter Stratigraphy 14:36–47

Faris M, El Hameed AT, Marzouk AM (1986) The Cretaceous/Tertiary boundary in Taramsa section, west of Qena, Nile Valley. Egypt Newsletters on Stratigraphy 16(2):85–97

Farouk S, Faris M (2013) Calcareous nannofossil and foraminiferal bio-events of the Danian-Selandian transition of the Quseir area, northwestern Red Sea margin. Egypt Micropaleontology 59:201–222

Firth JV, Wise SW Jr (1992) A preliminary study of the evolution of Chiasmolithus in the middle Eocene to Oligocene of Sites 647

and 748, ODP Leg 120. In Proceedings of the Ocean Drilling Program, Scientific Results 120:493–508
Geisen M, Bollmann J, Herrle J, Mutterlose J, Young J (1999) Calibration of the random settling technique for calculation of absolute abundances of calcareous nannofossil. Micropaleontology 45:437–442
Guasti E, Speijer RP, Brinkhuis H, Smit J, Steurbaut E (2006) Paleoenvironmental change at the Danian-Selandian transition in Tunisia: foraminifera, organic walled dinoflagellate cyst and calcareous nannofossil records. Mar Micropaleontol 59:210–229
Guasti E, Speijer RP, Fornaciari E, Schmitz B, Kroon D, Gharaibeh A (2005). Transient biotic change within the Danian–Selandian transition in Egypt and Jordan. In: Early Paleogene Environmental Turnover in the Southern Tethys as Recorded by Foraminiferal and Organic-walled Dinoflagellate Cysts Assemblages. Berichte aus dem Fachbereich Geowissenschaften der Universität Bremen 241:75–110
Hammer Ø, Harper DAT (2006) Paleontological data analysis. Blackwell
Hammer Ø, Harper DAT, Ryan PD (2001) PAST: paleontological statistics software package for education and data analysis. Palaeontol Electron 4:1–9
Haq BU, Lohmann GP (1976) Early Cenozoic calcareous nannoplankton biogeography of the Atlantic Ocean. Mar Micropaleontol 1:119–194
Hewaidy AGA, Farouk S, Bazeen YS (2019) The Selandian/Thanetian transition of the Naqb El-Rufuf section, Kharga Oasis, Western Desert, Egypt: foraminiferal biostratigraphy and sequence stratigraphy implications. J Afr Earth Sc 150:499–510
Hilting AK, Kump LR, Bralower TJ (2008) Variations in the oceanic vertical carbon isotope gradient and their implications for the Paleocene-Eocene biological pump. Paleoceanogr 23(3)
Hollis CJ, Naeher S, Clowes CD, Naafs BDA, Pancost RD, Taylor KW, Dahl J, Li X, Ventura GT, Sykes R (2022) Late Paleocene CO 2 drawdown, climatic cooling and terrestrial denudation in the southwest Pacific. Climate of the past 18(6):1295–1320
Jain S, Noori Jaff RB, Abdelhady AA (2022) Paleoenvironmental conditions across the Santonian/Campanian boundary: Inferences by calcareous nannofossils from Kurdistan region, northeastern Iraq. J African Earth Sci 188:104474. https://doi.org/10.1016/j.jafrearsci.2022.104474
Kasem AM, Faris M, Jovane L, Ads TA, Frontalini F, Zaky AS (2022) Biostratigraphy and paleoenvironmental reconstruction at the Gebel Nezzazat (Central Sinai, Egypt): a paleocene record for the Southern Tethys. Geosciences 12(2):96
Kassab W, Abdelhady AA (2022) Unitary Associations of the Aptian-Albian calcareous nannofossils of the Essaouira-Agadir Basin (NW Africa). Marine Micropaleontol 170:102076. https://doi.org/10.1016/j.marmicro.2021.102076
Kassab WG, Abdelhady AA, Ahmed MS, Abu Shama AA (2022) Early Cretaceous climate in North Africa: insights from the calcareous nannofossils in the Atlantic passive margin of Morocco. J Afr Earth Sc 197:104786
Keller G, Mateo P, Punekar J, Khozyem H, Gertsch B, Spangenberg J, Bitchong AM, Adatte T (2018) Environmental changes during the Cretaceous-Paleogene mass extinction and Paleocene-Eocene thermal maximum: implications for the Anthropocene. Gondwana Res 56:69–89
Legendre L, Legendre P (1983) Partitioning ordered variables into discrete states for discriminant analysis of ecological classifications. Can J Zool 61:1002–1010
Lüning S, Kuss J, Bachmann M, Marzouk AM, Morsi AM (1998) Sedimentary response to basin inversion: Mid Cretaceous-Early Tertiary pre-to syndeformational deposition at the Areif El Naqa anticline (Sinai, Egypt). Facies 38(1):103–136
Martini E (1971). Standard Tertiary and Quaternary calcareous nannoplankton zonation: Planktonic Conference. 2nd, Proceedings 2: 739–785
Metwally AA (2019) Characterization of the calcareous nannofossil assemblages across the Latest Danian Event (LDE) at Wadi El-Maheer, northern Eastern Desert. Egypt J African Earth Sci 156:58–67
Monechi S, Reale V, Bernaola G, Balestra B (2013) The Danian/Selandian boundaryat site 1262 (South Atlantic) and in the Tethyan region: biomagnetostratigraphy, evolutionary trends in fasciculiths and environmental effects of the latest Danian event. Mar Micropaleontol 98:28–40
Mutterlose J, Linnert C, Norris R (2007) Calcareous nannofossils from the Paleocene-Eocene Thermal Maximum of the equatorial Atlantic (ODP Site 1260B): evidence for tropical warming. Mar Micropaleontol 65(1–2):13–31
Obaidalla NA (2006). The Danian/Selandian (D/S) boundary event at Wadi Tarfa, north Eastern Desert, Egypt. In: Sixth International Conference on the Climate and Biota of the Early paleogene. Abstract 90
Obaidalla NA, El-Dawy MH, Kassab AS (2009) Biostratigraphy and paleoenvironment of the Danian/Selandian (D/S) transition in the Southern Tethys: a case study from north Eastern Desert. Egypt J Afr Earth Sci 53:1–15
Okada H, Bukry D (1980) Supplementary modification and introduction of code numbers to the low-latitude coccolith biostratigraphic zonation (Bukry, 1973; 1975). Mar Micropaleontol 5:321–325
Perch-Nielsen K (1985) Mesozoic calcareous nannofossils. In: Saunders P-N (ed) Bolli. Plankton stratigraphy. Cambridge University Press, Cambridge, pp 329–426
Petrizzo MR (2005) An early late Paleocene event on Shatsky Rise, northwest Pacific Ocean (ODP Leg 198): Evidence from planktonic foraminiferal assemblages. In Proceedings of the Ocean Drilling Program. Scientific Results, vol 198. Ocean Drilling Program
Pujalte V, Orue-Etxebarria X, Apellaniz E, Caballero F, Monechi S, Ortiz S, Schmitz B (2014) A prospective Early Late Paleocene event (ELPE) from the expanded Río Gor hemipelagic section (Betic Cordillera, southern Spain): foraminifera, nannofossil and isotopic data. Rendiconti Online Della Società Geologica Italiana 31:181–182
Quillévéré F, Aubry MP, Norris RD, Berggren WA (2002) Paleocene oceanography of the eastern subtropical Indian Ocean: An integrated magnetobiostratigraphic and stable isotope study of ODP Hole 761B (Wombat Plateau). Palaeogeogr Palaeoclimatol Palaeoecol 184(3–4):371–405
Raffi I, Backman J, Zachos JC, Sluijs A (2009) The response of calcareous nannofossil assemblages to the Paleocene Eocene Thermal Maximum at the Walvis Ridge in the South Atlantic. Marine Micropaleontology 703(4):201–212
Röhl U, Westerhold T, Bralower TJ, Petrizzo MR, Zachos JC (2004). An early late Paleocene global dissolution event and new constraints for an astronomically-tuned early Paleogene time scale, paper presented at 8th International Conference on Paleoceanography. Environ et Paleoenviron. Ocean Biarritz France
Romein AJT (1979). Lineages in early Paleogene calcareous nannoplankton (Doctoral dissertation, Utrecht University)
Said R (1962). The geology of Egypt. Elsevier, Amsterdam. 377
Said R (1990). Cenozoic. In: Said R (Editor), The geology of Egypt. A. A. Balkema/ Brookfield, Rotterdam, 48-451
Sayed MM, Abd El-Gaied IM, Abdelhady AA, Abd El-Aziz SM, Wagreich M (2022). Ostracods sensitivity to reconstructing water depths and oxygen levels: a case study from the Middle-Late Eocene of the Beni Suef area (Egypt). Marine Micropaleontol 102155. https://doi.org/10.1016/j.marmicro.2022.102155

Schmitz B, Pujalte V, Molina E, Monechi S, Orue-Etxebarria X, Speijer R, Alegret L, Apellaniz E, Arenillas I, Aubry MP, Baceta JI (2011) The global stratotype sections and points for the bases of the Selandian (Middle Paleocene) and Thanetian (Upper Paleocene) stages at Zumaia. Spain Episodes: International Geoscience Newsmagazine 34(4):220–243

Schoene B, Eddy MP, Samperton KM, Keller CB, Keller G, Adatte T, Khadri SF (2019) U-Pb constraints on pulsed eruption of the Deccan Traps across the end-Cretaceous mass extinction. Science 363(6429):862–866

Shahzad A, Khan J, Hanif M, Baumgartner-Mora C, Sarfraz Y, Ahmed KS, Riaz MT, Baumgartner PO, Wazir A (2023) Eocene nannofossils and paleoenvironmental reconstruction of the Kuldana Formation in Yadgar area, Muzaffarabad, northern Pakistan. Palaeoworld. https://doi.org/10.1016/j.palwor.2023.01.003

Shaker F, Kassab W (2022) Calcareous nannofossil biostratigraphy and paleoenvironmental study along the Upper Maastrichtian-Eocene sequence at Eastern and Western Deserts. Egypt J Afr Earth Sci 193:104583

Shackleton NJ, Backman J, Zimmerman HT, Kent DV, Hall MA, Roberts DG, Schnitker D, Baldauf JG, Desprairies A, Homrighausen R, Huddlestun P (1984) Oxygen isotope calibration of the onset of ice-rafting and history of glaciation in the North Atlantic region. Nature 307(5952):620–623

Soliman MF, Obaidalla NA (2006). Danian/Sealndian (D/S) boundary at Gabal Abu Had Section, Nile Valley (Egypt); lithostratigraphy, mineralogy, geochemistry and biostratigraphy. In: Sixth International Conference on the Climate and Biota of the Early paleogene. Abstract, 125

Soliman MF, Obaidalla NA (2010) Danian-Selandian transition at Gabal el-Qreiya section, Nile Valley (Egypt): lithostratigraphy, biostratigraphy, mineralogy and geochemistry. N Jb Geol Paläont 258:1–30

Speijer RP (2003) Danian-Selandian sea-level change and biotic excursion on the southern Tethyan margin (Egypt). In: Wing SL, Gingerich PD, Schmitz B, Thomas E (Eds.), Causes and Consequences of Globally Warm Climates in the Early Paleogene, Geological Society of America Special Paper 369: 275–290

Speijer RP, Schmitz B (1998) A benthic foraminiferal record of Paleocene sea level and trophic/redox conditions at Gebel Aweina. Egypt. Palaeogeogr Palaeoclimatol Palaeoecol 137(1–2):79–101

Sprong J, Speijer RP, Steurbaut E (2009) Biostratigraphy of the Danian/Selandian transition in the southern Tethys, with special reference to the Lowest Occurrence of planktic foraminifera Igorina albeari. Geol Acta 7:63–77

Sprong J, Youssef MA, Bornemann A, Schulte P, Steurbaut E, Stassen P, Kouwenhoven TJ, Speijer RP (2011) A multi-proxy record of the Latest Danian Event at Gebel Qreiya, Eastern Desert. Egypt J Micropaleontol 30:167–182

Sprong J, Kouwenhoven TJ, Bornemann A, Dupuis C, Speijer RP, Stassen P, Steurbaut E (2013) In search of the Latest Danian Event in a paleobathymetric transect off Kasserine Island, north-central Tunisia. Palaeogeogr Palaeoclimatol Palaeoecol 379:1–16

Sprong J, Guasti E, Fornaciari E, Youssef AM, Schulte P, Speijer RP (2006). Paleoenvironmental and sea level change of the Nile Valley Basin (Egypt) at the Danian/Selandian transition. In: Sixth International Conference on the Climate and Biota of the Early Paleogene. Abstract, 128

Tantawy AA (2003) Calcareous nannofossil biostratigraphy and paleoecologyof the cretaceous-tertiary transition in the central eastern desert of Egypt. Mar Micropaleontol 47(3–4):323–356

Thomsen E, Heilmann-Clausen C (1985) The Danian-Selandian boundary at Svejstrup with remarks on the biostratigraphy of the boundary in western Denmark. Bull Geol Soc Den 33:341–362

Varol O (1989). Paleocene calcareous nannofossil biostratigraphy. In: Crux JA, van Heck SE (Eds.), Nannofossils and Their Applications. British Micropaleontology Society Series, 12: 267–310

Wei W, Wise SW Jr (1990) Biogeographic gradients of middle Eocene-Oligocene calcareous nannoplankton in the South Atlantic Ocean. Palaeogeogr Palaeoclimatol Palaeoecol 79(1–2):29–61

Westerhold T, Röhl U, Raffi I et al (2008) Astronomical calibration of the Paleocene time. Palaeogeogr Palaeoclimatol Palaeoecol 257:377–403

Westerhold T, Röhl U, Donner B, McCarren HK, Zachos JC (2011) A complete high-resolution Paleocene benthic stable isotope record for the central Pacific (ODP Site 1209). Paleoceanography 26(2)

Youssef M (2003). Micropaleontological and stratigraphical analyses of the Late Cretaceous/Early Tertiary succession of the Southern Nile Valley (Egypt), Ruhr-Universität Bochum, Germany. Published online, Ph. D. Thesis. http//: www.netahtml/Hss/Diss/MohamedMohamedYoussefAli/diss. Pdf.

Zachos JC, Wara MW, Bohaty S, Delaney MI, Petrizzo MR, Brill A, Bralowere TJ, Premoli Silva I (2003) A transient rise in tropical sea surface temperature during the Paleocene-Eocene Thermal Maximum. Science 203:1551–1554